Two-Stage Control System of a DC Motor using Dual-Sampling Observer

Hiromitsu Ogawa, Ryo Tanaka, Takahiro Murakami, Yoshihisa Ishida

Department of Electronics and Bioinformatics, Meiji University
Japan (Tel:+81-44-934-7305; corresponding e-mail: h_ogawa@meiji.ac.jp).

Abstract: This study describes a two-stage control system using a dual-sampling method based on an optimal control scheme. The system consists of a speed-control system and a position-control system: the speed is controlled before the changeover point; after the changeover point, the position is controlled. For low speed and low sensor resolution, the proposed method uses position data estimated by an observer. The proposed method can control a plant with a low sensor resolution, unlike the conventional method, which has random oscillation in this situation. This method is confirmed through a simulation and by implementing a DC motor control.

Keywords: Optimal Control, Speed Control, Position Control, Motor Control, Two-Stage Control

1. INTRODUCTION

Today, almost all consumers are interested in small devices with as many attractive functions as possible. To fulfill increasing customer requirements, manufacturers seek to discover high-precision processing technologies for manufacturing these devices. Especially, electronics manufacturers use many DC motors; therefore, the DC motor with highly accurate control impacts the possibility of a manufactured device that fits their needs. Under these circumstances, advanced control systems are attracting much interest among engineers. However, advanced control is difficult to apply because of system hardware and software restrictions, e.g., plant input limitations. Under these restrictions, the system plant control performance is reduced. To overcome these concerns, several control methods have been proposed (Youbin Peng et al., 1996; Y. X. Su et al., 2005; Tai-Sik Hwang et al., 2007; Ming-Yang Cheng et al., 2007; Rong-Jong Wai et al., 2007; Da Zhang et al., 2008; Jong-Woo Choi et al., 2009).

In the area of motion control, a two-stage control method consisting of a position-control and speed-control method has been proposed as one of the concepts (Katsuhisa Endo et al., 1990). In this method, the speed of the plant output is controlled before the changeover point. After the changeover point, the position of the plant output is controlled. The two-stage control method changes the control from the speed to the position of the plant output when the position of the plant output exceeds the threshold value. The distance of the position control is independent of the position set point; as a result, overshoot of the plant output is unaffected by the set point. In other words, engineers can design and control the overshoot of the plant output without concerns for the set point. However, this two-stage control uses the same controlled parameters during speed control and position control. Thus, engineers need to consider the fair tradeoff between speed control and position control. Moreover, this method has a steady-state error when the plant has a disturbance.

To overcome these concerns, two-stage control based on an optimal control method for a position-control system and a speed-control system has been proposed (Hiromitsu Ogawa et al., 2010). In this system, both speed-control and position-control parameters are designed by an optimal control method, respectively. This means that the speed-control system design is independent of the position-control system design. The engineer can control the overshoot of the plant output speed. However, in the case of low speed with low sensor resolution, the plant output is a random oscillation. Dealing with low-speed and low-sensor-resolution situations is one of the attractive problems in the control area, and some approaches have been proposed actively (Hiroshi Fujimoto et al., 2005; Chin-Sheng Chen et al., 2008). One of the approaches is to use the process data only when the plant output is updated. During non-updated plant output, the system does not use the plant output for the system feedbacks.

This study describes the proposed method, a two-stage control system with a disturbance observer, using a dual-sampling approach, for the control of a DC motor. The key feature of the proposed method is the changeover system, which shifts from speed control to position control continuously. The effectiveness of the proposed method is shown in the simulation and the experimental results of DC motor control.

2. TWO-STAGE CONTROL

The two-stage control system uses the optimal control theory for controlled parameter design. The optimal control theory helps engineers to choose the controlled parameters rather than choosing the parameters by trial and error. The task of designing an optimal control system is an important and a complex problem, and the two-stage control system design by optimal control theory contributes to a solution. Let us consider the single input and the single output of a plant as follows:

$$G(s) = \frac{Y(s)}{U(s)} = \frac{b}{s(s+a)}, \tag{1}$$

where $U(s)$ and $Y(s)$ are plant input and output respectively, and a and b are as follows:

$$a = \frac{{k_m}^2}{J_{eq}R_m}, \ b = \frac{k_m}{J_{eq}R_m}, \tag{2}$$

where J_{eq} is the inertia moment, k_m is the motor torque, and R_m is the armature resistance. The system discretized by zero-order hold is as follows:

$$\boldsymbol{x}(k+1) = \boldsymbol{A}\boldsymbol{x}(k) + \boldsymbol{B}u(k), \tag{3}$$

$$y(k) = \boldsymbol{C}\boldsymbol{x}(k), \tag{4}$$

where the state variables are as follows:

$$\boldsymbol{x}(k) = \begin{bmatrix} x_1(k) & x_2(k) \end{bmatrix}^{\mathrm{T}}, \tag{5}$$

where $x_1(k)$ is a plant position and $x_2(k)$ is a plant speed. Then, let us consider the augmented plant as follows:

$$\begin{bmatrix} \boldsymbol{\Delta x}(k+1) \\ e(k) \end{bmatrix} = \begin{bmatrix} A & 0 \\ -C & 1 \end{bmatrix} \begin{bmatrix} \boldsymbol{\Delta x}(k) \\ e(k-1) \end{bmatrix} + \begin{bmatrix} B \\ 0 \end{bmatrix} \Delta u(k), \tag{6}$$

$$e(k) = r(k) - y(k), \tag{7}$$

$$\boldsymbol{\Delta x}(k) = \boldsymbol{x}(k) - \boldsymbol{x}(k-1), \tag{8}$$

$$\Delta u(k) = u(k) - u(k-1). \tag{9}$$

The performance criterion is used in practice for quadratic optimal control formulation:

$$J = \sum_{k=0}^{\infty} \{ e(k-1)Qe(k-1) + \Delta u(k) R \Delta u(k) \}, \tag{10}$$

where Q is a positive-semi definite real symmetric matrix and R is a positive-definite real symmetric matrix. In this study, Q and R represent the scalar quantity. So the plant input during the position-control is represented as follows:

$$\Delta u(k) = \begin{bmatrix} \boldsymbol{F_3} & F_4 \end{bmatrix} \begin{bmatrix} \boldsymbol{\Delta x}(k) \\ e(k-1) \end{bmatrix}. \tag{11}$$

The speed-control system is designed by the optimal control method the same as is the position-control system. Each gain ($\boldsymbol{F_1}$, F_2) is obtained for the speed-control.

Then, let us design the changeover point. The changeover point is designed so that the system changes the control from speed to position continually. To design the changeover point easily, the plant input at the changeover point is defined as follows:

$$u(m) = \boldsymbol{F_3}\boldsymbol{x}(m) - M(m) + F_4 \sum_{i=0}^{m-1} e(i) - h(m), \tag{12}$$

where m is the time of the changeover point and $M(m)$ and $h(m)$ are defined so that the plant input is the same at the changeover point as follows:

$$M(m) = \boldsymbol{F_3}\boldsymbol{x}(m) - \boldsymbol{F_1}\boldsymbol{x}(m), \tag{13}$$

$$h(m) = (F_4 - F_2) \sum_{i=0}^{m-1} e(i). \tag{14}$$

The state variables of the plant at the changeover point are as follows:

$$\begin{aligned} \boldsymbol{x}(m+1) &= \begin{bmatrix} x_1(m+1) & x_2(m+1) \end{bmatrix}^{\mathrm{T}}, \\ &= \begin{bmatrix} x_1(m) + v \cdot T_s & v \end{bmatrix}^{\mathrm{T}}, \end{aligned} \tag{15}$$

$$\boldsymbol{F}_3 = \begin{bmatrix} F_{31} & F_{32} \end{bmatrix}^{\mathrm{T}}, \tag{16}$$

where v is the set point of the speed and T_s is the sampling time. The plant input after the changeover point is as follows:

$$u(m+1) = u(m) - F_{31} \cdot v \cdot T_s + F_4 \cdot l, \tag{17}$$

where l is the error between the position set point and the plant output position at the changeover point. Then, the value of the plant input before the changeover point is defined as the same value as that of the plant input after the changeover point. The following equation is obtained:

$$l \approx \frac{F_{31} \cdot v \cdot T_s}{F_4}. \tag{18}$$

If the system satisfies the above equation, it changes the control from speed to position. Moreover, (18) contains the current speed and sampling time for each gain, so the system does not depend on the initial position and speed.

3. DUAL-SAMPLING OBSERVER

The plant output is not updated at every sampling time if a controlled plant with low sensor resolution moves slowly. For example, when the plant output is position and the plant speed is calculated from the plant output position, the system is unstable. The system generates feedback with a plant output and speed that are different from the real plant output and speed. The dual-sampling observer uses the plant output at the updated plant output. In this study, the time variable is as defined in Fig. 1. Then, the following equation is obtained:

$$k = \sum_{i=1}^{m} n_i + p. \tag{19}$$

When p equals zero, the dual-sampling observer uses the plant output so that the dual-sampling observer feedback the error between plant output and its observer output. It means the plant output is almost same as real plant output. When p

does not equal zero, it does not use the plant output for its feedback, because the plant output is not same as real plant output. So the dual-sampling observer does away with the non-real plant output for its feedback. The observer converges to the correct one. Fig. 2 shows the proposed system. When the system controls the speed, the switch is set to (i). When the system controls the position, the switch is set to (ii). $V(z)$, $R(z)$, $Y(z)$, $G(z)$, and each parameter ($\boldsymbol{F_1}$, F_2, $\boldsymbol{F_3}$, and F_4) are a set point of the speed, a set point of the position, a plant output, a plant, and the gains that were calculated in Section 2, respectively. Let us consider a single input and a single output of the plant as follows:

$$\begin{aligned}\boldsymbol{x}(\sum_{i=1}^{m} n_i + p + 1) &= \boldsymbol{A}\boldsymbol{x}(\sum_{i=1}^{m} n_i + p) \\ &+ \boldsymbol{B}u(\sum_{i=1}^{m} n_i + p) + \boldsymbol{G_g}w(\sum_{i=1}^{m} n_i + p),\end{aligned} \tag{20}$$

$$y(\sum_{i=1}^{m} n_i + p) = \boldsymbol{C}\boldsymbol{x}(\sum_{i=1}^{m} n_i + p) + d(\sum_{i=1}^{m} n_i + p), \tag{21}$$

where $\boldsymbol{G_g}$ is the disturbance matrix, w is the process noise, and d is the output disturbance. Then, the augmented plant is as follows:

$$\begin{aligned}\begin{bmatrix}\boldsymbol{x}(\sum_{i=1}^{m} n_i + p + 1) \\ w(\sum_{i=1}^{m} n_i + p + 1)\end{bmatrix} &= \begin{bmatrix}\boldsymbol{A} & \boldsymbol{G_g} \\ 0 & 1\end{bmatrix}\begin{bmatrix}\boldsymbol{x}(\sum_{i=1}^{m} n_i + p) \\ w(\sum_{i=1}^{m} n_i + p)\end{bmatrix} \\ &+ \begin{bmatrix}\boldsymbol{B} \\ 0\end{bmatrix}u(\sum_{i=1}^{m} n_i + p) \\ &= \boldsymbol{A_m}\boldsymbol{x_m}(\sum_{i=1}^{m} n_i + p) + \boldsymbol{B_m}u(\sum_{i=1}^{m} n_i + p),\end{aligned} \tag{22}$$

$$\begin{aligned}y(\sum_{i=1}^{m} n_i + p) &= \begin{bmatrix}\boldsymbol{C} & 0\end{bmatrix}\begin{bmatrix}\boldsymbol{x}(\sum_{i=1}^{m} n_i + p) \\ w(\sum_{i=1}^{m} n_i + p)\end{bmatrix} + d(\sum_{i=1}^{m} n_i + p) \\ &= \boldsymbol{C_m}\boldsymbol{x_m}(\sum_{i=1}^{m} n_i + p) + d(\sum_{i=1}^{m} n_i + p).\end{aligned} \tag{23}$$

Next, let us consider applying the Kalman filter with the dual-sampling theory. The dual-sampling observer uses the plant output at the updated plant output as follows:

(The case of $p = 0$: the plant output is updated)

$$\begin{aligned}\boldsymbol{x_m}(\sum_{i=1}^{m} n_i + p + 1) &= \boldsymbol{A_m}\boldsymbol{x_m}(\sum_{i=1}^{m} n_i + p) + \boldsymbol{B_m}u(\sum_{i=1}^{m} n_i + p) \\ &+ \boldsymbol{K}\left[y(\sum_{i=1}^{m} n_i + p) - \boldsymbol{C_m}\boldsymbol{x_m}(\sum_{i=1}^{m} n_i + p)\right]\end{aligned} \tag{24}$$

(The case of $p = 1, 2, 3, \ldots$: the plant output is not updated)

$$\boldsymbol{x_m}(\sum_{i=1}^{m} n_i + p + 1) = \boldsymbol{A_m}\boldsymbol{x_m}(\sum_{i=1}^{m} n_i + p) + \boldsymbol{B_m}u(\sum_{i=1}^{m} n_i + p) \tag{25}$$

(For case of $p = 0, 1, 2, 3, \ldots$, the observer output is independent with the updated plant output timing)

$$y_m(\sum_{i=1}^{m} n_i + p) = \boldsymbol{C_m}\boldsymbol{x_m}(\sum_{i=1}^{m} n_i + p) + d(\sum_{i=1}^{m} n_i + p), \tag{26}$$

The above observer, a dual-sampling observer based on the Kalman filter and the disturbance observer, uses the plant output, when the plant output is updated ($p = 0$).

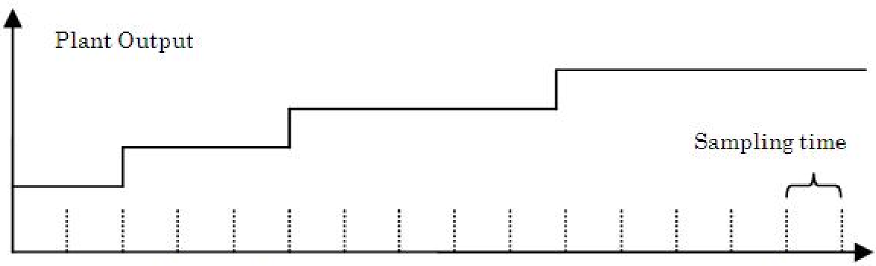

k		0	1	2	3	4	5	6	7	8	9	10	11	12	13	14	....
p		0	1	0	1	2	0	1	2	3	4	0	1	2	3	4	....
n	n_1	0	0	2	2	2	2	2	2	2	2	2	2	2	2	2	....
	n_2	0	0	0	0	0	3	3	3	3	3	3	3	3	3	3	....
	n_3	0	0	0	0	0	0	0	0	0	0	5	5	5	5	5	....
	....	....	....	....	....	....	....	....	....	....	....	....	....	....	....	....	....

Fig. 1. Redefinition of the sampling rate.

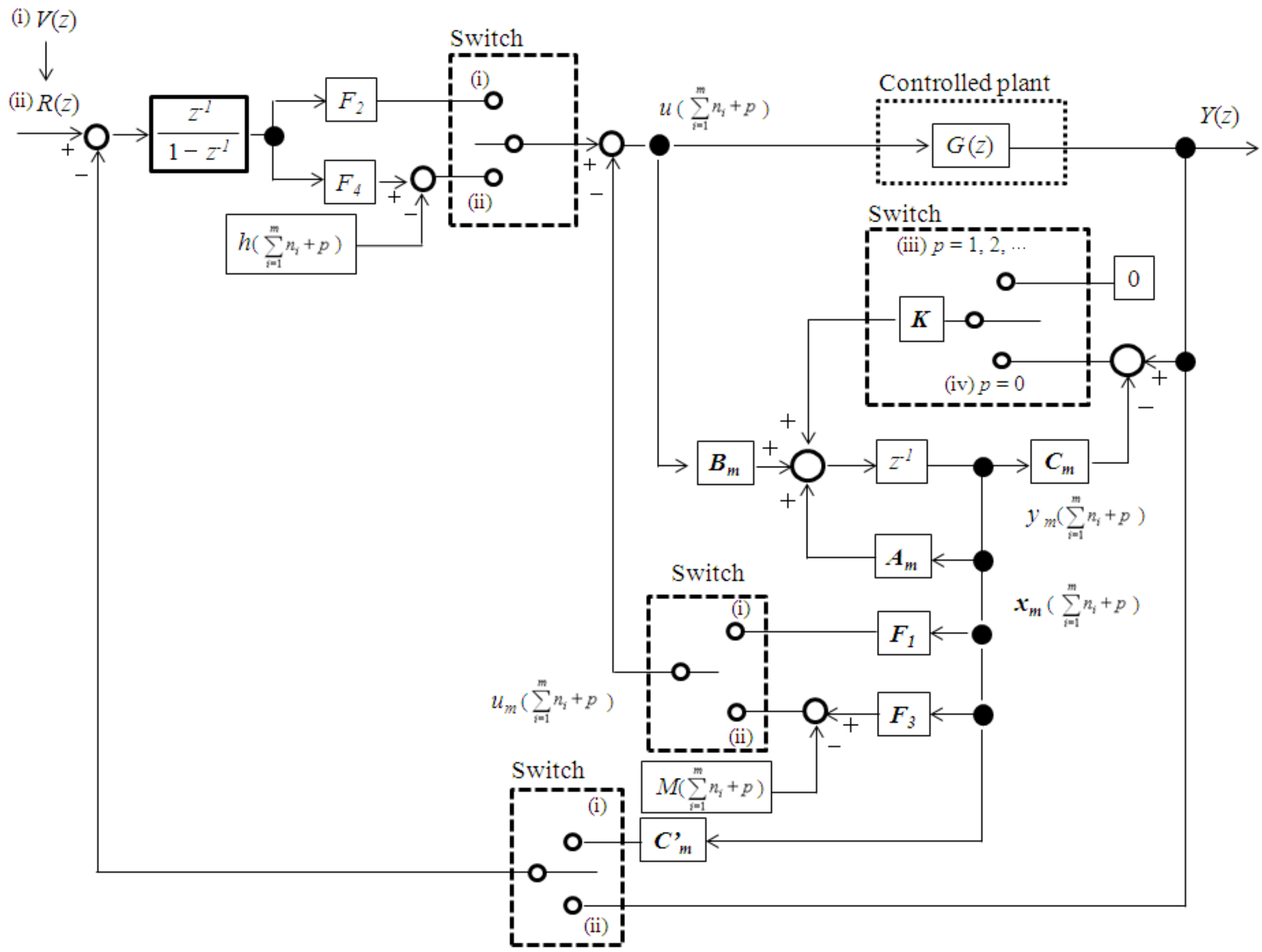

Fig. 2. Proposed method.

4. CONTROL SYSTEM

Fig. 3 shows the block diagram of the control system. The control method is installed in the controller. And the controller outputs the manipulated value that calculated by the control method to the D/A Converter (AD5430-02A) manufactured by AND Co., LTD. Then, the D/A Converter outputs the analog voltage to the DC motor (DCMCT) manufactured by Quanser Co. LTD. The Angular speed of DC motor is controlled by voltage level. It means that the DC motor stops when the voltage level is zero. The encoder generates the pulse (Phase A and Phase B) based on the angle of the DC motor. And the counter (AD5430-11) manufactured by AND Co. LTD. counts the leading edge of the pulse (Phase A and Phase B) and trailing edge of the pulse (Phase A and Phase B). When the counter detects the leading edge of the pulse (Phase A) and then detects the leading edge of the pulse (Phase B) or when the counter detects the trailing edge of the pulse (Phase A) and then detects the trailing edge of the pulse (Phase B), the counter increases its count (value) by each edge. When the counter detects the leading edge of the pulse (Phase A) and then detects the trailing edge of the pulse (Phase B) or when the counter detects the trailing edge of the pulse (Phase A) and then detects the leading edge of the pulse (Phase B), the counter decreases its count (value) by each edge. Then, the controller receives the count as the Angle of the DC motor.

Fig. 4 shows the DC motor. The DC motor has the inertia load disc. Its diameter is 0.0496 [m] and its weight is 0.068 [kg]. The purpose of this study is to control a low-cost DC motor. So the torque of the DC motor control is not objective.

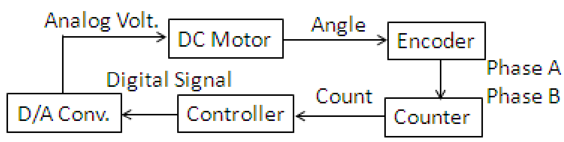

Fig. 3. Block diagram of the control system.

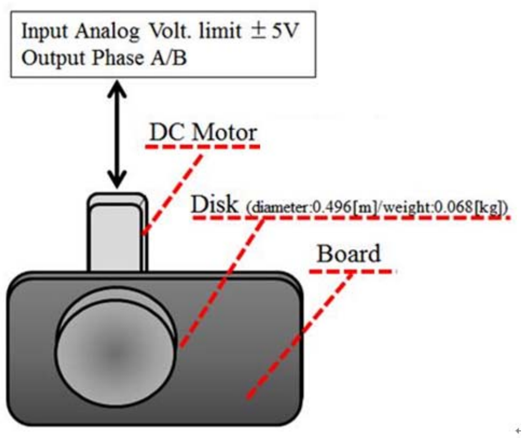

Fig. 4. DC motor.

5. SIMULATION AND EXPERIMENTAL RESUTLS

5.1. Simulation Results 1

This experiment shows that the proposed method can control a plant with low sensor resolution, although the conventional method cannot do so.

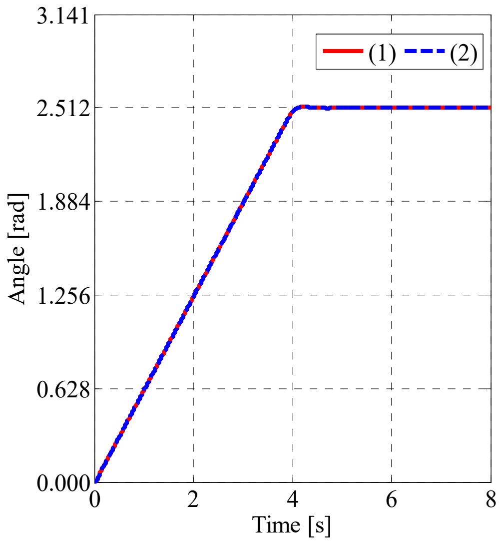

(1) Conventional method: no sensor resolution

(2) Proposed method: no sensor resolution

Fig. 5. Plant position result.

Let us consider the following known second-order plant:

$$G(s) = \frac{159}{s(s+14.0)} \tag{27}$$

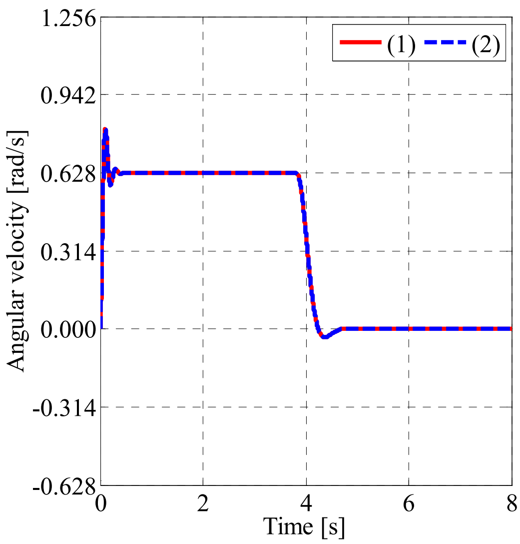

(1) Conventional method: no sensor resolution

(2) Proposed method: no sensor resolution

Fig. 6. Plant angular velocity result.

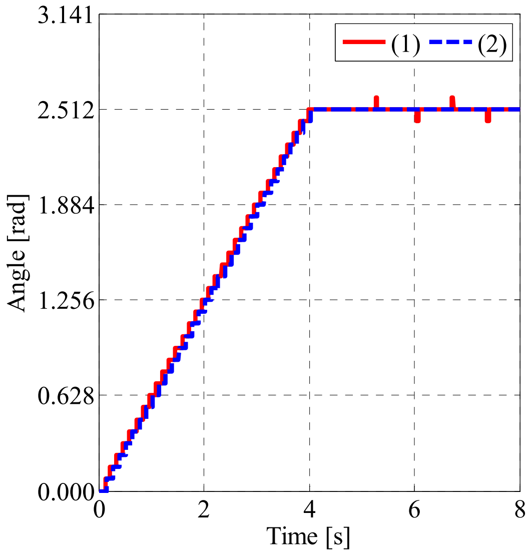

(1) Conventional method: sensor resolution 0.0785 [rad/count]

(2) Proposed method: sensor resolution 0.0785 [rad/count]

Fig. 7. Plant position result.

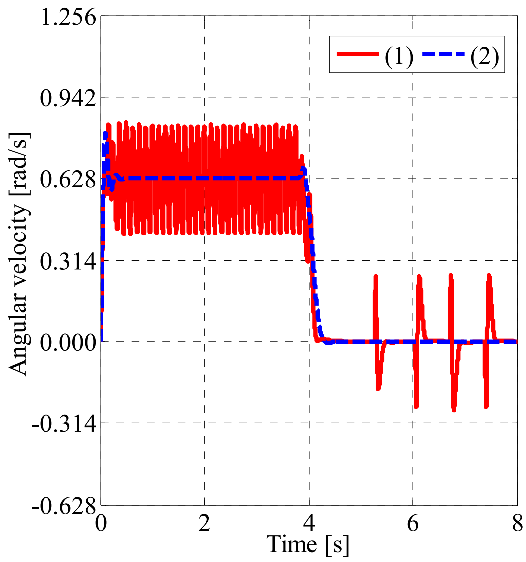

(1) Conventional method: sensor resolution 0.0785 [rad/count]

(2) Proposed method: sensor resolution 0.0785 [rad/count]

Fig. 8. Plant angular velocity result.

The set point of the speed is 0.628 [rad/s] and the set point of the position is 2.512 [rad]. And the Q/R is 1 both for speed control and for position control. The disturbance matrix is used experientially as follows:

$$\boldsymbol{G_g} = \begin{bmatrix} 0.000 & 0.009 & 0.010 \end{bmatrix}^{\mathrm{T}} \tag{28}$$

Figs. 5 and 6 show the simulation results for position and speed, respectively in the case of no sensor resolution as ideal situation. Figs. 7 and 8 show the simulation results for the position and aped respectively in the case of sensor resolution 0.0785 [rad/count] as actual situation. Both conventional method and proposed method can control the plant in the case of no sensor resolution, but in the case of sensor resolution 0.0785 [rad/count], the proposed method can control and the conventional method cannot control the plant due to sensor resolution.

5.2. Simulation Results 2

This experiment shows that the proposed method can control a plant with low sensor resolution, although the conventional method is unstable. Let us consider the following known second-order plant:

$$G(s) = \frac{159}{s\left(s+14.0\right)} \tag{29}$$

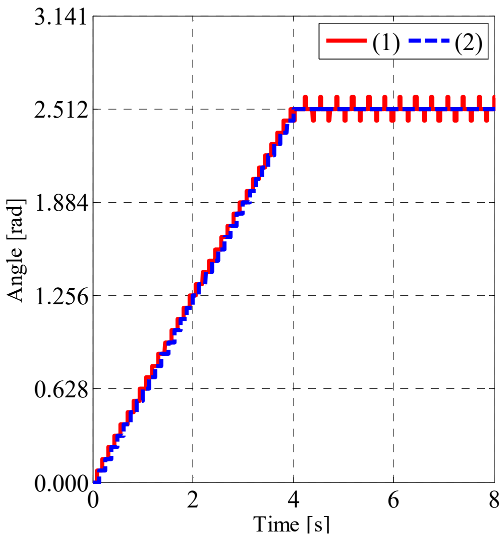

(1) Plant position of the conventional method

(2) Plant position of the proposed method

Fig. 9. Optimal control design: speed $Q/R = 1$, position $Q/R = 0.1$.

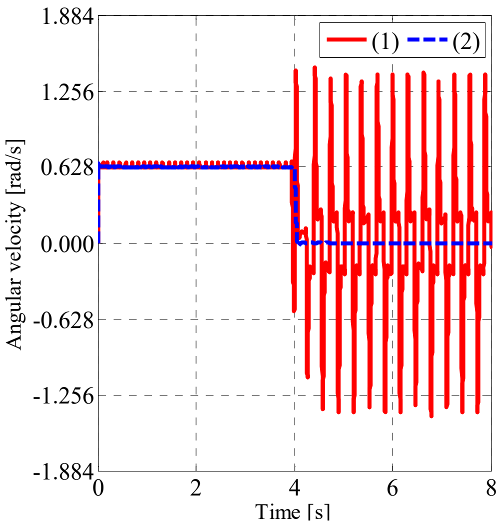

(1) Plant velocity of the conventional method

(2) Plant velocity of the proposed method

Fig. 10. Optimal control design: speed $Q/R = 1$, position $Q/R = 0.1$.

The set point of the speed is 0.628 [rad/s] and the set point of the position is 2.512 [rad].

The disturbance matrix is used experientially as follows:

$$\boldsymbol{G}_g = \left[0.000 \quad 0.009 \quad 0.010\right]^{\mathrm{T}} \tag{30}$$

The sensor resolution is 0.1534 [rad/count]. Figs. 9 and 10 show the case of $Q/R = 1$ for speed control and $Q/R = 0.1$ for position control. Figs. 11 and 12 show the case of $Q/R = 1$ for speed control and $Q/R = 1$ for position control. Figs. 13 and 14 show the case of $Q/R = 1$ for speed control and $Q/R = 10$ for position control.

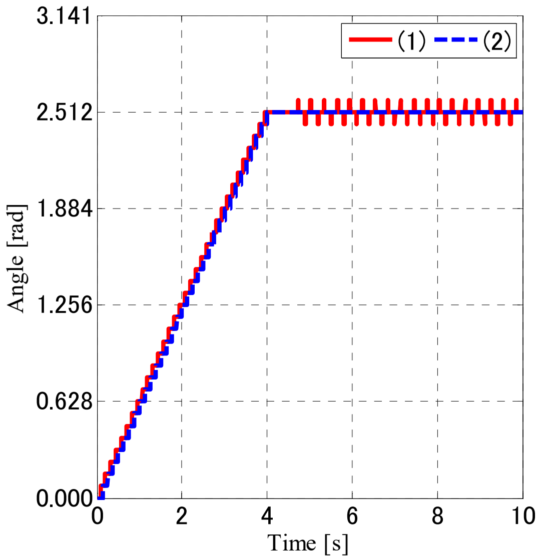

(1) Plant position of the conventional method

(2) Plant position of the proposed method

Fig. 11. Optimal control design: speed $Q/R = 1$, position $Q/R = 1$.

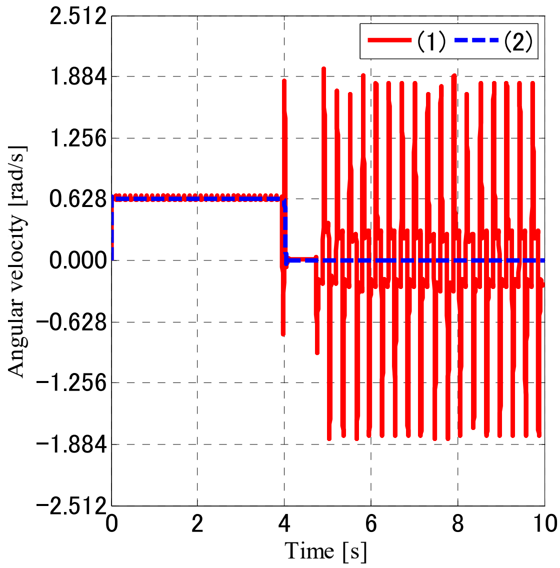

(1) Plant velocity of the conventional method

(2) Plant velocity of the proposed method

Fig. 12. Optimal control design: speed $Q/R = 1$, position $Q/R = 1$.

From Figs. 9 through 14, the proposed method is confirmed to control the plant, although the conventional method has random oscillation, and it is independent of the design of Q/R for position.

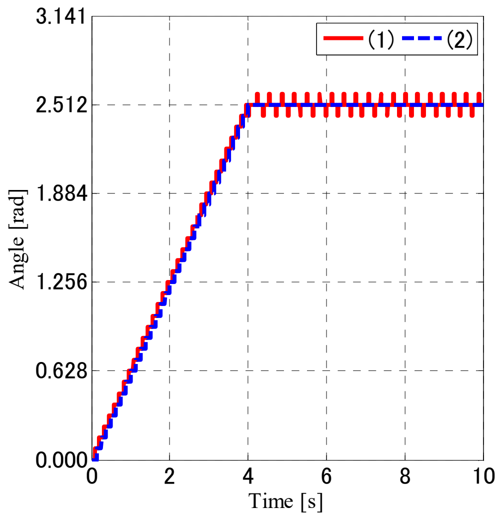

(1) Plant position of the conventional method

(2) Plant position of the proposed method

Fig. 13. Optimal control design: speed $Q/R = 1$, position $Q/R = 10$.

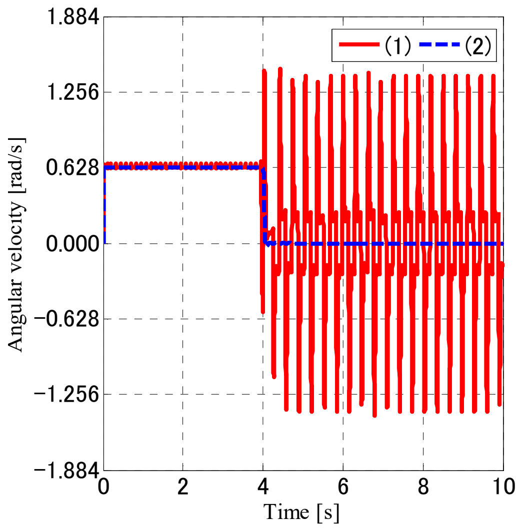

(1) Plant velocity of the conventional method

(2) Plant velocity of the proposed method

Fig. 14. Optimal control design: speed $Q/R = 1$, position $Q/R = 10$.

5.3. DC Motor Control Results

This experiment shows that the proposed method can control a DC motor with low sensor resolution. The sampling rate is 10 [ms]. The set point of the angle is 25.1 [rad] and the set point of the angular velocity is 1.534 [rad/s]. The Q/R is 1 both for speed control and for position control. Figs. 15 and 16 show the DC motor control results for position and speed, respectively. The proposed method can control the plant with low sensor resolution, while the conventional method cannot do so. The main reason for this result is that the proposed method uses the plant output when the plant output is updated. This means that the proposed method uses the plant output when it is the veritable value. Conversely, the conventional method uses the plant output at every sampling time, although the plant output is not updated because of low sensor resolution. This means that, because it cannot use the veritable plant output, the conventional method is unstable.

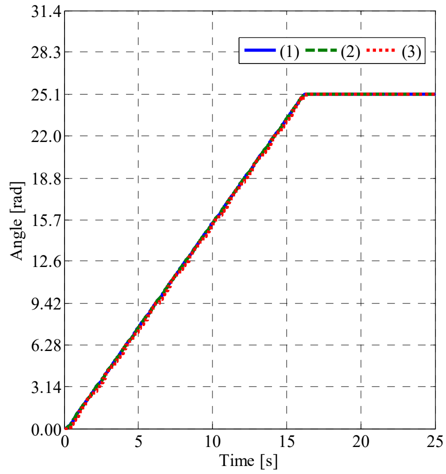

(1) Conventional method: sensor resolution 1.534×10^{-3} [rad/count]

(2) Proposed method: sensor resolution 1.534×10^{-3} [rad/count]

(3) Proposed method: the sensor resolution 0.1534 [rad/count]

* The result of conventional method that has the sensor resolution 0.1534 [rad/count] is removed from the Fig. 15 to show others clearly, because the result of this conventional method is unstable.

Fig. 15. Plant position result.

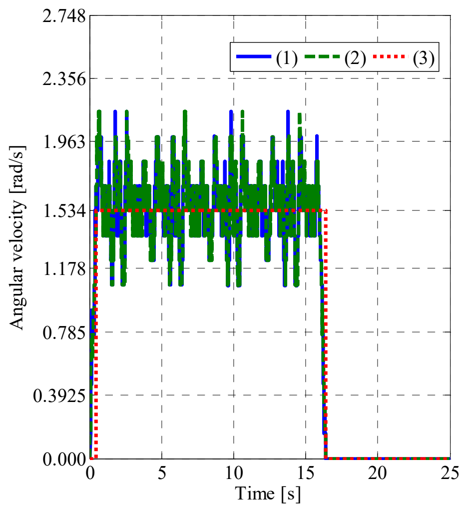

(1) Conventional method: sensor resolution 1.534×10^{-3} [rad/count]

(2) Proposed method: sensor resolution 1.534×10^{-3} [rad/count]

(3) Proposed method: the sensor resolution 0.1534 [rad/count]

* The result of conventional method that has the sensor resolution 0.1534 [rad/count] is removed from the Fig. 16 to show others clearly, because the result of this conventional method is unstable.

Fig. 16. Plant angular velocity result.

6. CONCLUSIONS

In this study, two-stage control based on an optimal control scheme with a dual-sampling observer is proposed. Two-stage control consists of speed and position control. The dual-sampling observer is revised when the controlled plant output is updated. This control scheme can therefore be applied to a plant that has low sensor resolution when the plant working speed is slowed. Successful application of the proposed system on a DC motor with low sensor resolution is confirmed.

REFERENCES

Chin-Sheng Chen and Ying-Tsung Teng, (2008). Multirate Digital Servo Drive Based on Acceleration Observer and Disturbance Compensator, *17th World Congress of the International Federation of Automation Control Seoul*, Vol. 17, pp. 9278-9283.

Da Zhang and Hui Li, (2008). A Stochastic-Based FPGA Controller for an Induction Motor Drive With Integrated Neural Network Algorithm, *IEEE Transactions on Industrial Electronics*, Vol. 55, pp. 551-561.

Hiromitsu Ogawa, Manato Ono, Naohiro Ban, and Yoshihisa Ishida, (2010). Two Stage Control of a DC Motor Using an Optimal Control Scheme, *SICE Transactions on paper industry*, Vol. 9, pp. 120-126.

Hiroshi Fujimoto and Bin Yao, (2005). Multirate Adaptive Robust Control for Discrete-Time Non-Minimum Phase Systems and Application to Linear Motors, *IEEE/ASME Transactions on MECHATRONICS*, Vol. 10, pp. 371-377.

Jong-Woo Choi and Sang-Cheol Lee, (2009). Antiwindup Strategy for PI-Type Speed Controller, *IEEE Transactions on Industrial Electronics*, Vol. 56, pp. 2039-2046.

Katsuhisa Endo, Yoshihisa Ishida, Takashi Honda, and Yasuo Ogawa, (1990). Digital control of a pneumatic cylinder, *SICE Transactions*, Vol. 26, pp. 397-404.

Ming-Yang Cheng and Cheng-Chien Lee, (2007). Motion Controller Design for Contour-Following Tasks Based on Real-Time Contour Error Estimation, *IEEE Transactions on Industrial Electronics*, Vol. 54, pp. 1686-1695.

Rong-Jong Wai and Chia-Chin Chu, (2007). Motion Control of Linear Induction Motor via Petri Fuzzy Neural Network, *IEEE Transactions on Industrial Electronics*, Vol. 54, pp. 281-295.

Tai-Sik Hwang and Jul-Ki Seok, (2007). Observer-Based Ripple Force Compensation for Linear Hybrid Stepping Motor Drives, *IEEE Transaction on Industrial Electronics*, Vol. 54, pp. 2417-2424.

Y. X. Su, C. H. Zheng, and B. Y. Duan, (2005). Automatic Disturbances Rejection Controller for Precise Motion Control of Permanent-Magnet Synchronous Motors, *IEEE Transactions on Industrial Electronics*, Vol. 52, pp. 814-823.

Youbin Peng, Damir Vrancic, and Raymond Hanus, (1996). Anti-windup, Bumpless, and Conditioned Transfer Techniques for PID Controllers, *IEEE Control Systems,* Vol. 16, pp. 48-57.